Dimension of Dirac modes in IR phase

Xiao-Lan Meng

Collaborators: Yi-bo Yang, Peng Sun, Andrei Alexandru,
Ivan Horvath, Keh-Fei Liu, and Gen Wang

Outline

- 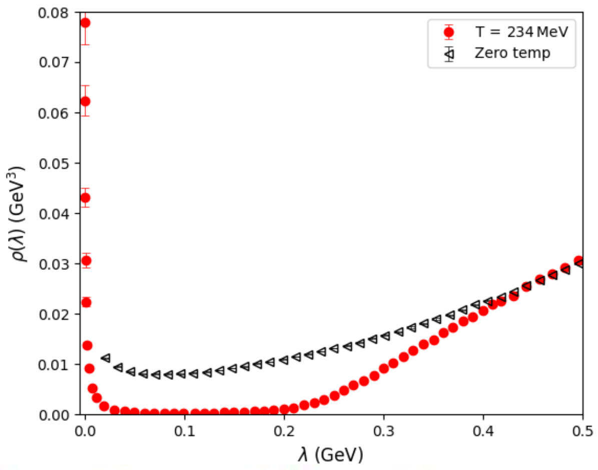

Dirac spectrum above crossover;

- Dimension of Dirac Eigenvectors…

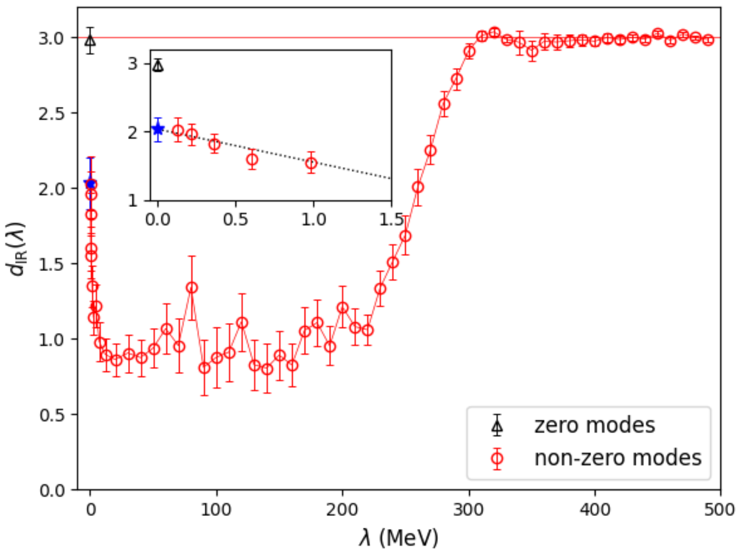

- 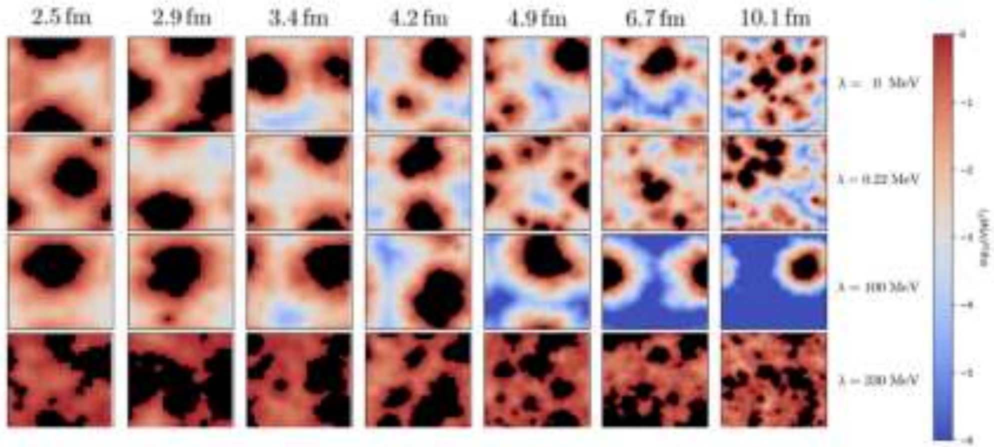

…and its distribution.

Dirac spectrum

at zero temperature

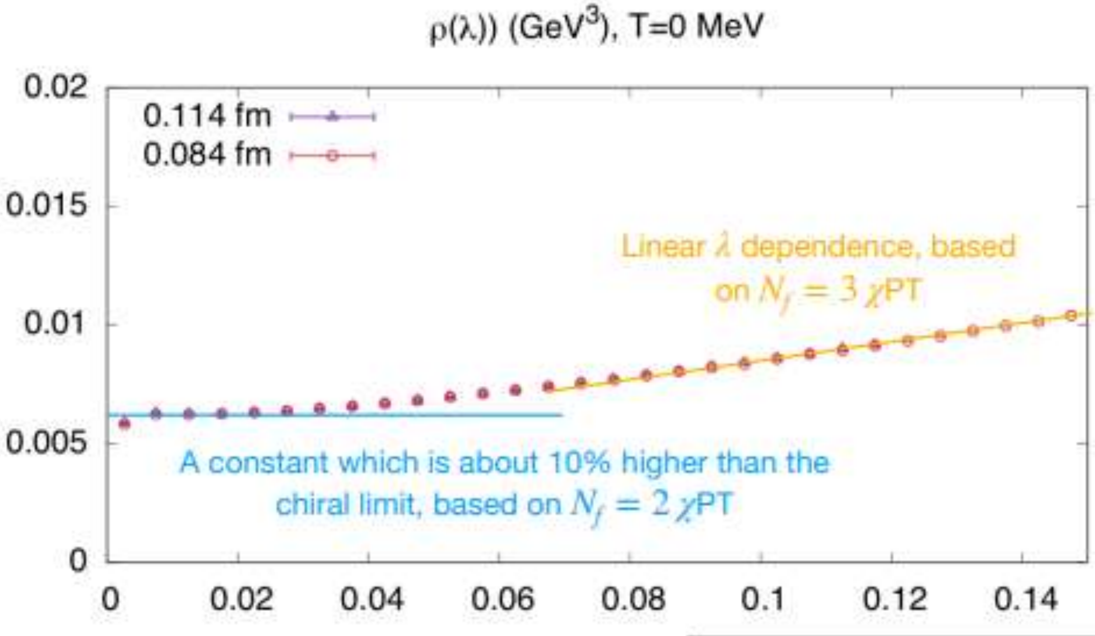

J. Liang, et.al, χQCD, arXiv:2102.05380

$$\rho(\lambda, V) = \frac{\Sigma}{\pi}\left(1 + \frac{N_f^2 - 4}{N_f}\frac{\lambda\Sigma}{32\pi F^4}\right) + \mathcal{O}\left(\frac{1}{\sqrt{V}}, m_q^{\mathrm{sea}}, \lambda^2\right)$$

P. H. Damgaard and H Fukaya, JHEP01(2009),052, 0812.2797

- 2+1 flavors DWF ensembles at physical light quark masses and two lattice spacings.
- Dirac spectrum based on the exact eigensolver of the overlap fermion.
- Corresponds to the chiral condensate in proper limits: $-\langle\bar{\psi}\psi\rangle = \pi \lim_{\lambda\to 0}\lim_{m_l\to 0}\lim_{V\to\infty} \rho(\lambda, V, m_l)$.

Dirac spectrum

above the crossover temperature

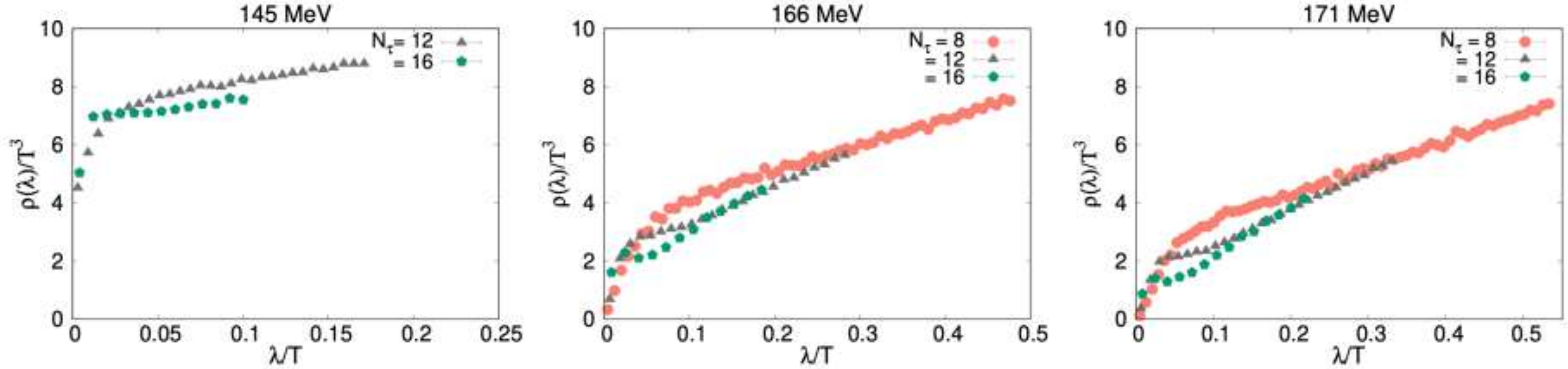

- 2+1 flavors HISQ ensembles at physical light quark masses and 2-3 lattice spacings:
- Dirac spectrum with unitary HISQ action.
- $\rho(\lambda \to 0)$ becomes lower with higher temperature.
- $\rho(\lambda)$ develops a peaked structure at small λ, which becomes sharper as $a \to 0$.

O. Kaczmarek, et.al., arXiv: 2301.11610

Dirac spectrum

above the crossover temperature

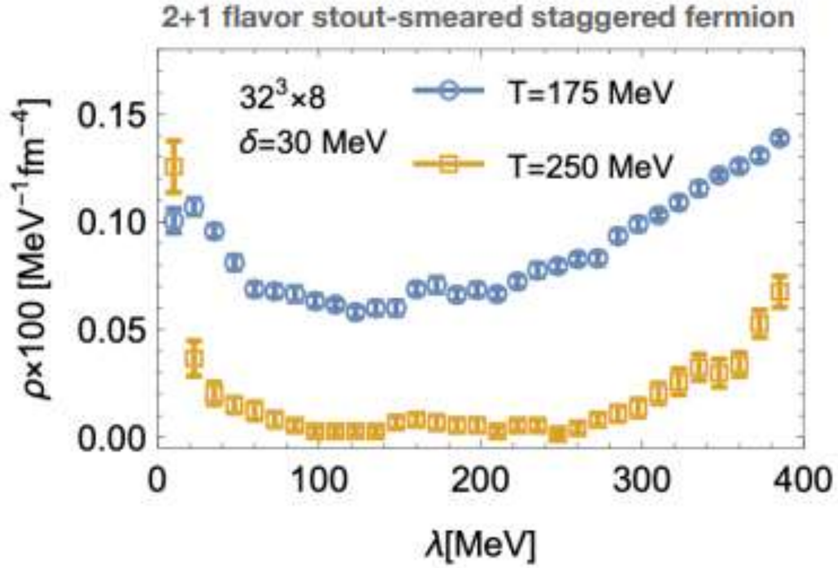

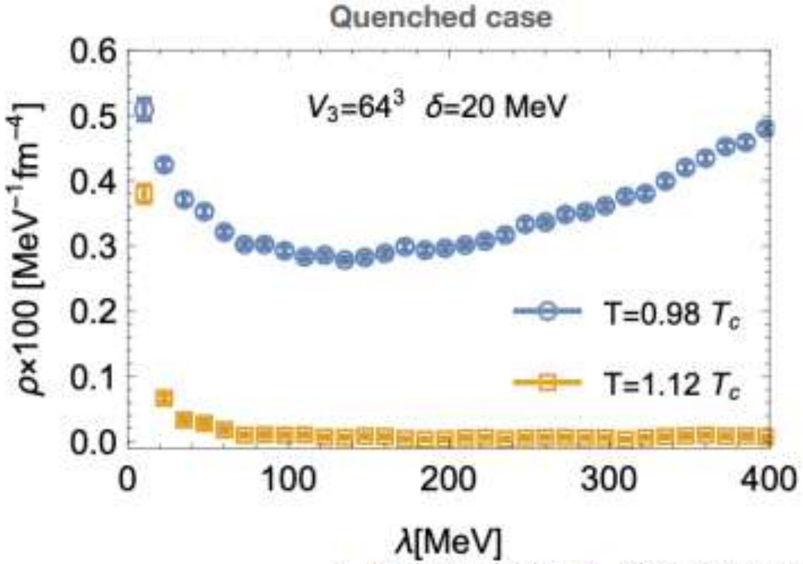

A. Alexandru, I. Horvath., Phys.Rev.D 100 (2019) 094507

- Both the quenched and 2+1 flavor cases:
- Dirac spectrum using overlap fermion shows obvious IR peak at $T >$ 200 MeV.
- The IR peak seems to be much larger than the unitary HISQ case.

Dirac spectrum

above the crossover temperature

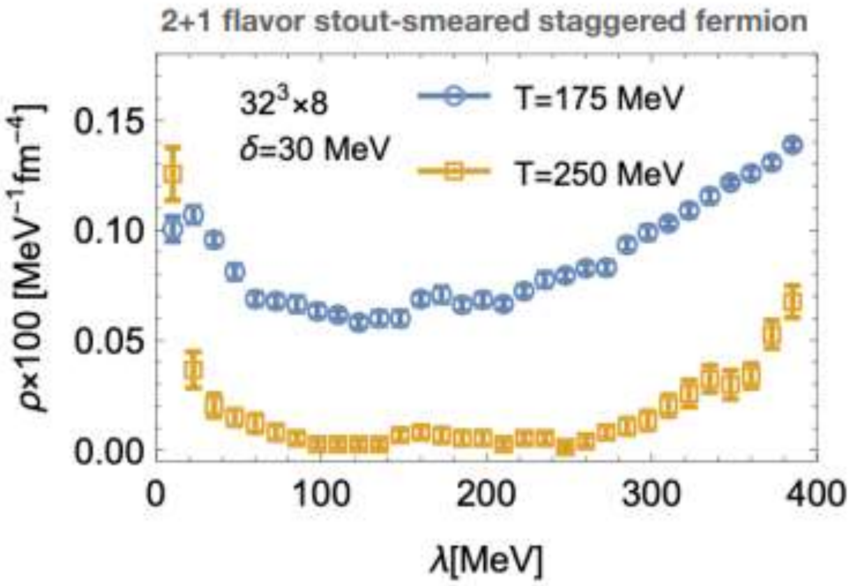

A. Alexandru, I. Horvath., Phys.Rev.D 100 (2019) 094507

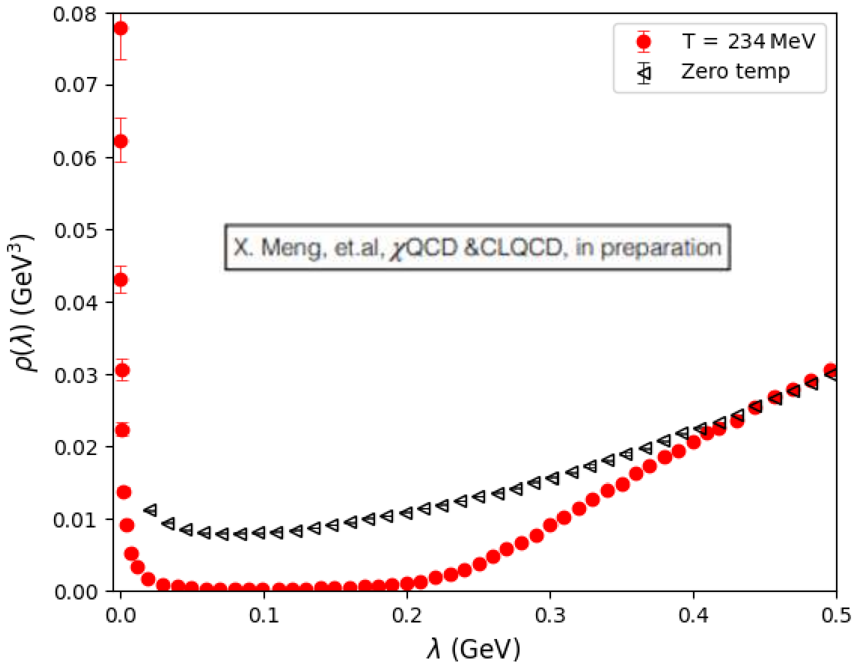

- Dirac spectrum using overlap valence fermion and clover sea is somehow similar to that using staggered fermion sea.

Possible new phase

of thermal QCD

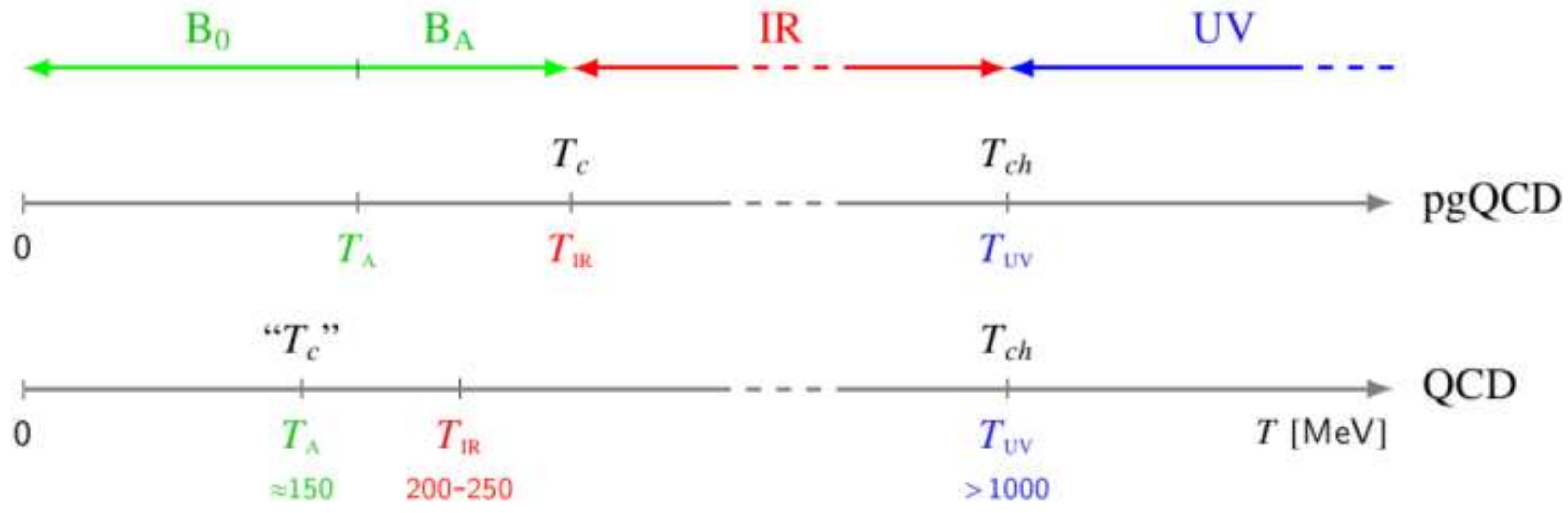

- Above T_{IR}: $\rho(\lambda) \propto 1/\lambda$ at $\lambda < T$ and then scale invariance at long distance;
- Above T_{UV}: $\rho(\lambda) \sim 0$ at $\lambda < T$ and then only a weakly interacting gluon plasma remains.

A. Alexandru, I. Horvath, Phys.Rev.D 100 (2019) 094507

Possible new phase

of thermal QCD

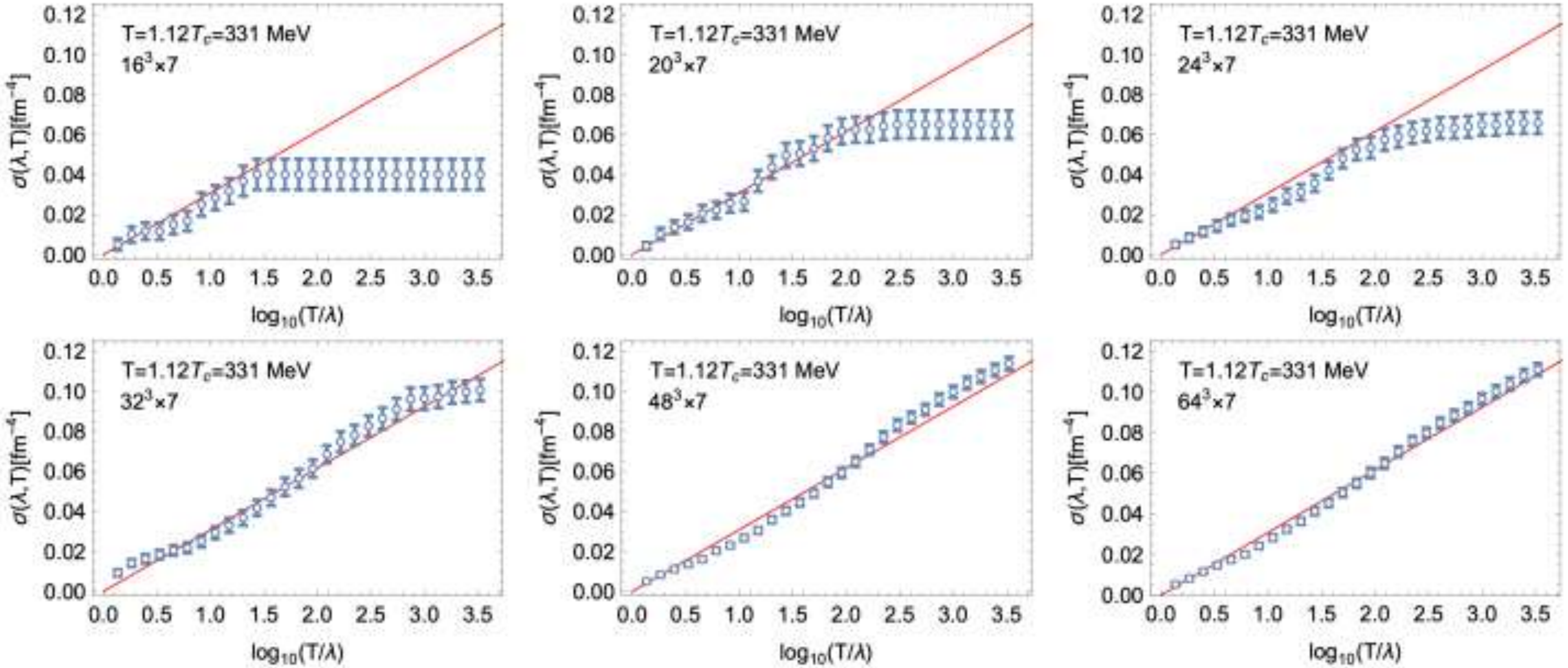

- Above $T_{\rm IR}$: $\rho(\lambda) \propto 1/\lambda$ at $\lambda < T$ and then scale invariance at long distance;
- In such a case, $\sigma(\lambda, T) \equiv \int_\lambda^T \rho(\omega)\mathrm{d}\omega \propto \ln\dfrac{\lambda}{T}$ down to some $\lambda_{\rm IR} \propto 1/L$.
- But if the IR peak suffers from the action sensitivities, is there any other criteria?

A. Alexandru, I. Horvath, Phys.Rev.D 100 (2019) 094507

Dirac spectrum

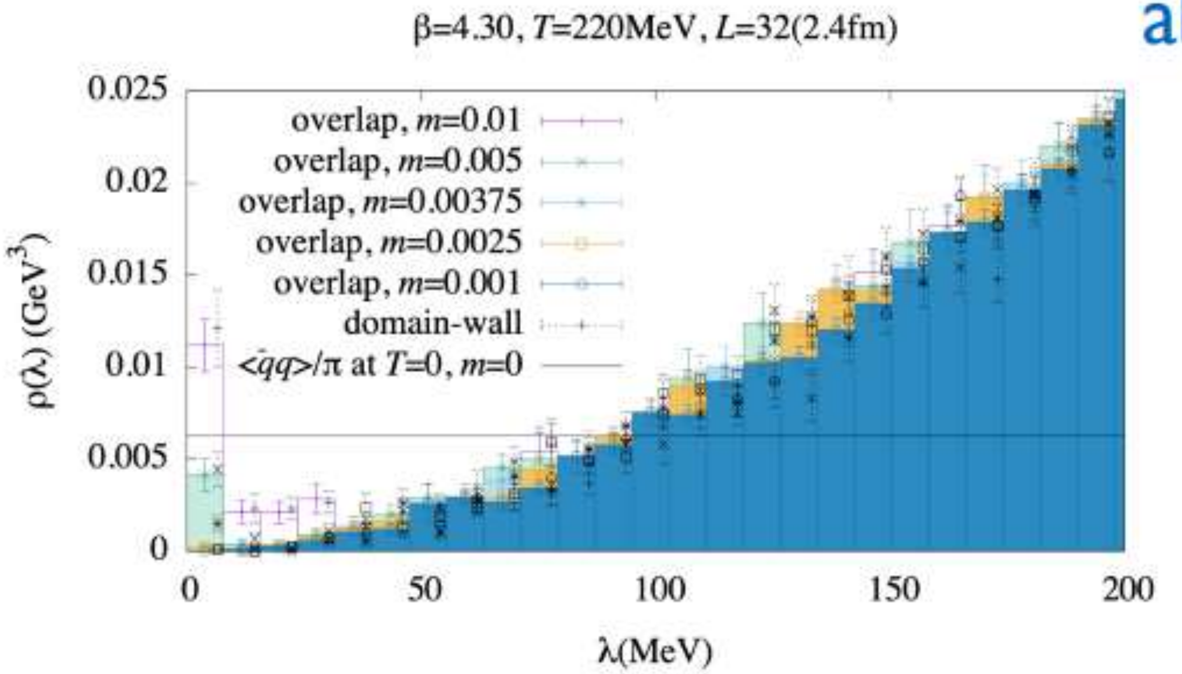

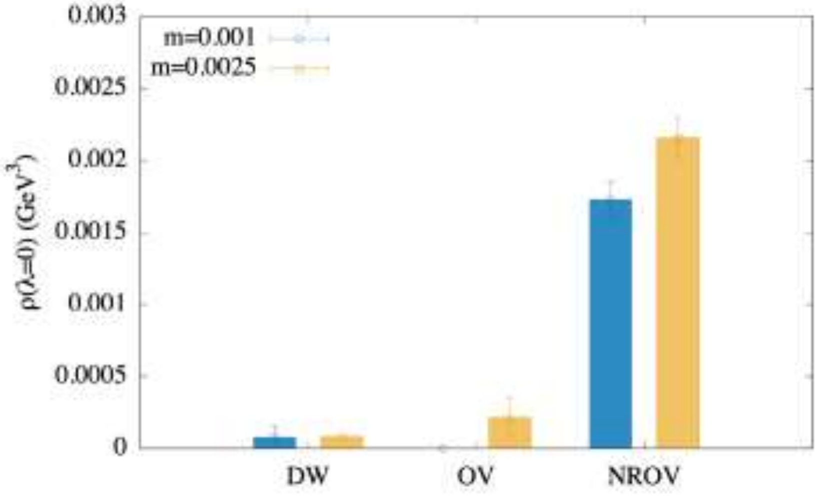

above the crossover temperature

- 2 flavors DWF ensembles with different light quark masses.
- The IR peak using overlap valence fermion is sizable before reweighting;
- That using DWF is much smaller;
- And almost vanishes if we use the overlap valence fermion and reweight the DWF sea to overlap sea.

S. Aoki, et.al., JLQCD, Phys.Rev.D103 (2021) 074506

Dirac spectrum

and mixed action effects

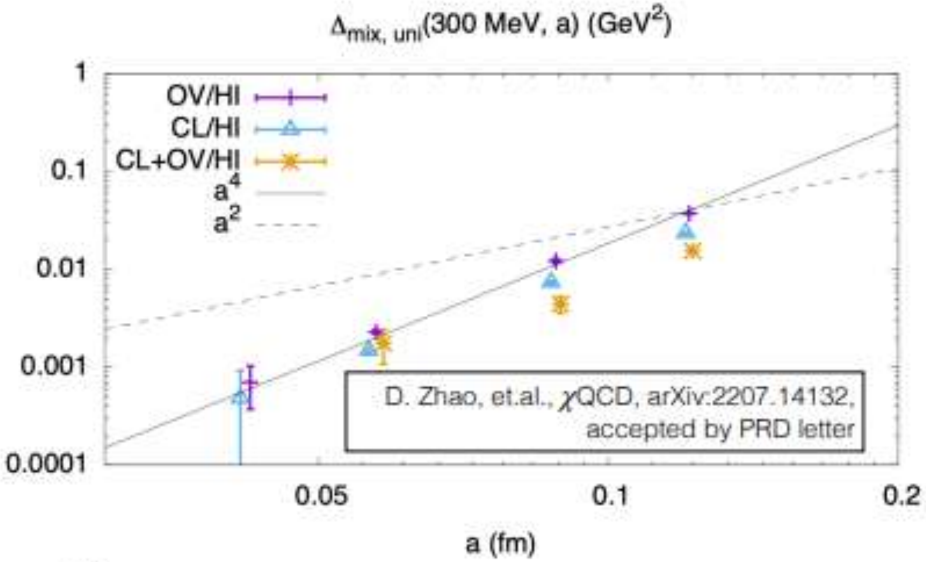

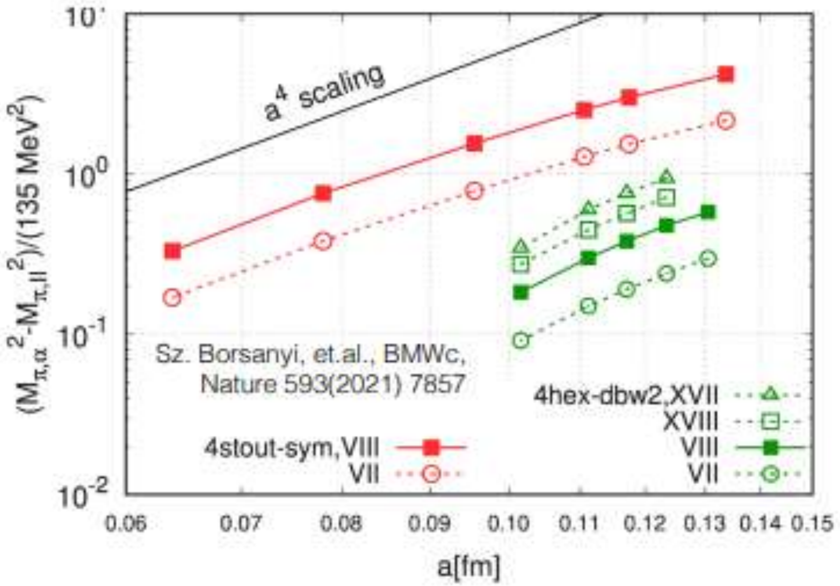

- The difference in the IR peak with different setups would be recognized as mixed action or taste mixing effect.
- Both the mixed action and taste mixing effects would be $\mathcal{O}(a^4)$, based on present results with various valence and sea actions at multiple lattice spacings.
- Proper continuum extrapolation should be essential to reach the final answer.

Dirac spectrum

at different lattice spacings

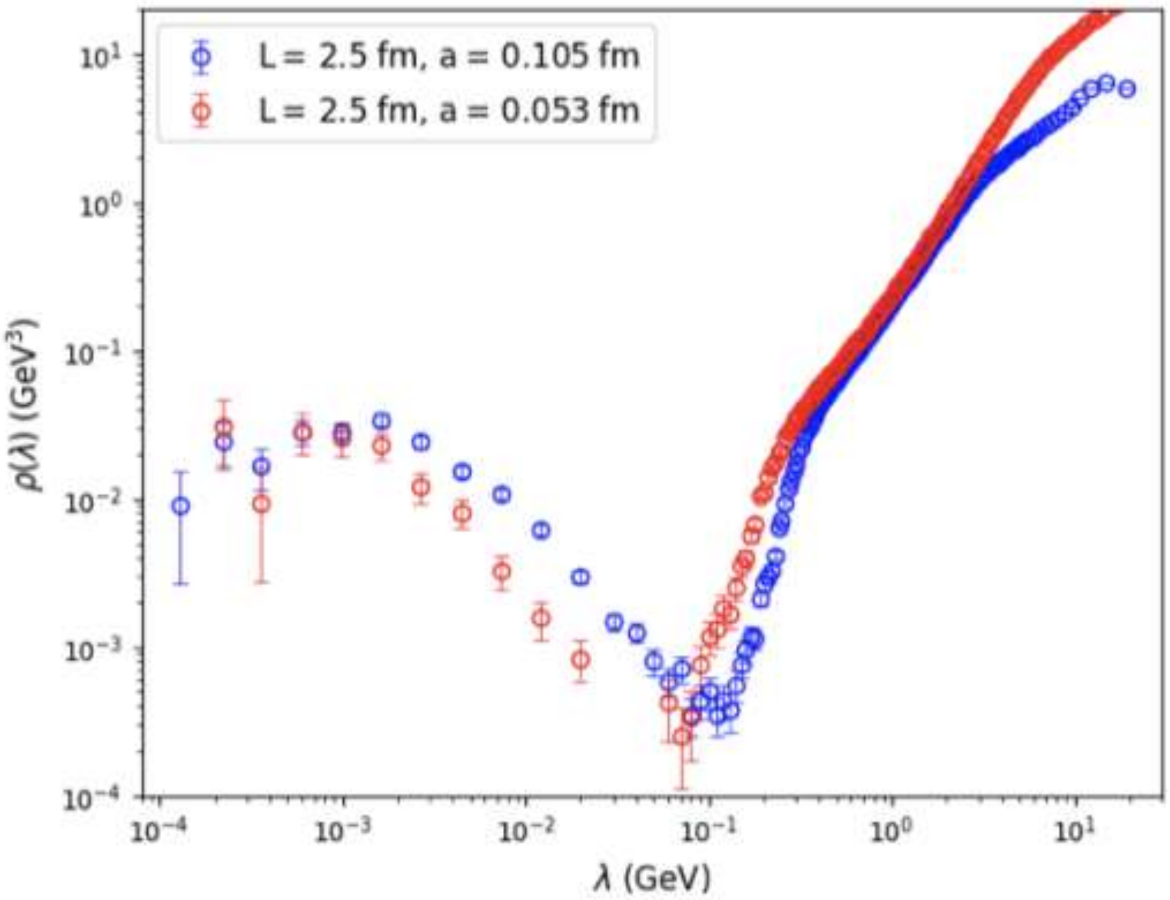

- $N_f = 2 + 1$, $T = 234$ MeV.
- Valence: overlap fermion on 1-step HYP smeared gauge;
- Sea: Tadpole improved Clover fermion with stout smearing;
- Tadpole improved Symanzik gauge.
- The IR peak remains at smaller lattice spacing, while narrower.

Dirac spectrum

and overlap fermion

- The overlap fermion operator satisfies the Ginsburg-Wilson,

$$\gamma_5 D_{ov} + D_{ov}\gamma_5 = \frac{a}{\rho} D_{ov}\gamma_5 D_{ov}$$

- It can be rewritten into

$$D_{ov}^{-1}\gamma_5 + \gamma_5 D_{ov}^{-1} = \frac{a}{\rho}\gamma_5, \quad (D_{ov}^{-1} - \frac{1}{2\rho})\gamma_5 + \gamma_5(D_{ov}^{-1} - \frac{1}{2\rho}) = 0$$

- Thus the chiral fermion operator satisfying $\gamma_5 D_c = -D_c\gamma_5$ can be defined through the overlap fermion operator:

$$D_c + m_q = \frac{D_{ov}}{1 - \frac{1}{2\rho}D_{ov}} + m_q,\ D_{ov} = \rho(1 + \gamma_5 \epsilon_{ov}(\rho))\,.$$

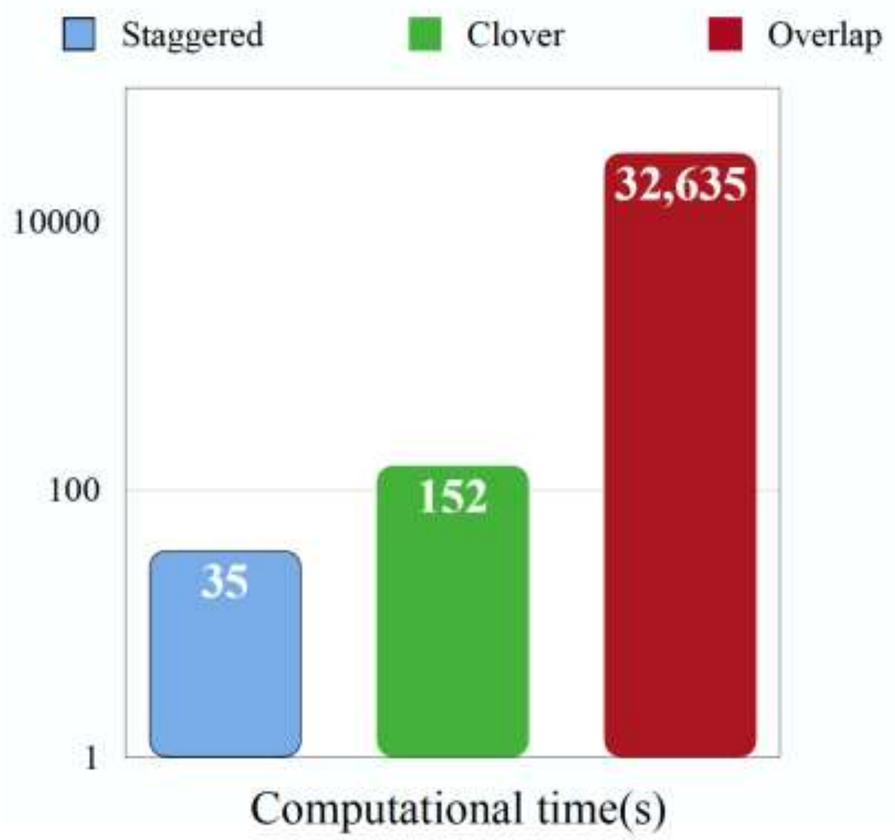

Dirac spectrum

overlap fermion v.s. staggered fermion

- The non-zero and finite modes of the overlap fermion are paired, $D_{\rm ov}v_{\rm ov} = \lambda_{\rm ov}v_{\rm ov}$, $D_{\rm ov}\gamma_5 v_{\rm ov} = \lambda_{\rm ov}^{*}\gamma_5 v_{\rm ov}$;
- And then we have $Dv = \lambda v$, $D\gamma_5 v = \lambda^{*}\gamma_5 v = -\lambda\gamma_5 v$, $Dv_{L/R} = \lambda v_{R/L}$ and also $|v_L| = |v_R|$;
- The exact zero modes have given chiral sector, $1 = |v_{L/R}| \gg |v_{R/L}| = 0$, and $\sum_{\lambda=0} (v_\lambda)^\dagger \gamma_5 v_\lambda = Q$.
- Thus the exact zero modes and non-zero modes of the overlap fermion are quite different from each other.

T.W. Chiu, Phys.Rev.D 60 (1999) 034503

- All the modes of the staggered fermion are also paired, $D^{\rm st}v^{\rm st} = \lambda^{\rm st}v^{\rm st}$, $D^{\rm st}\gamma_5 v^{\rm st} = -\lambda^{\rm st}\gamma_5 v^{\rm st}$;
- $v^{\rm st}_{L/R}$ corresponds to even/odd sites of the eigenvector, and then $Dv_{L/R} = \lambda v_{R/L}$ is quite natural.
- But $|v_L|$ and $|v_R|$ on each configuration can be different, to allow the topological charge $Q^{\rm st} \equiv \sum_{-{\rm i}M<\lambda<{\rm i}M} (v_\lambda^{\rm st})^\dagger \gamma_5 v_\lambda^{\rm st} = \sum_{-{\rm i}M<\lambda<{\rm i}M} (|v_{\lambda,L}|^2 - |v_{\lambda,R}|^2)$ to be non-zero.

C. Bonanno, et.al., JHEP 10 (2019) 187

Measure-based dimension

of the eigenvectors

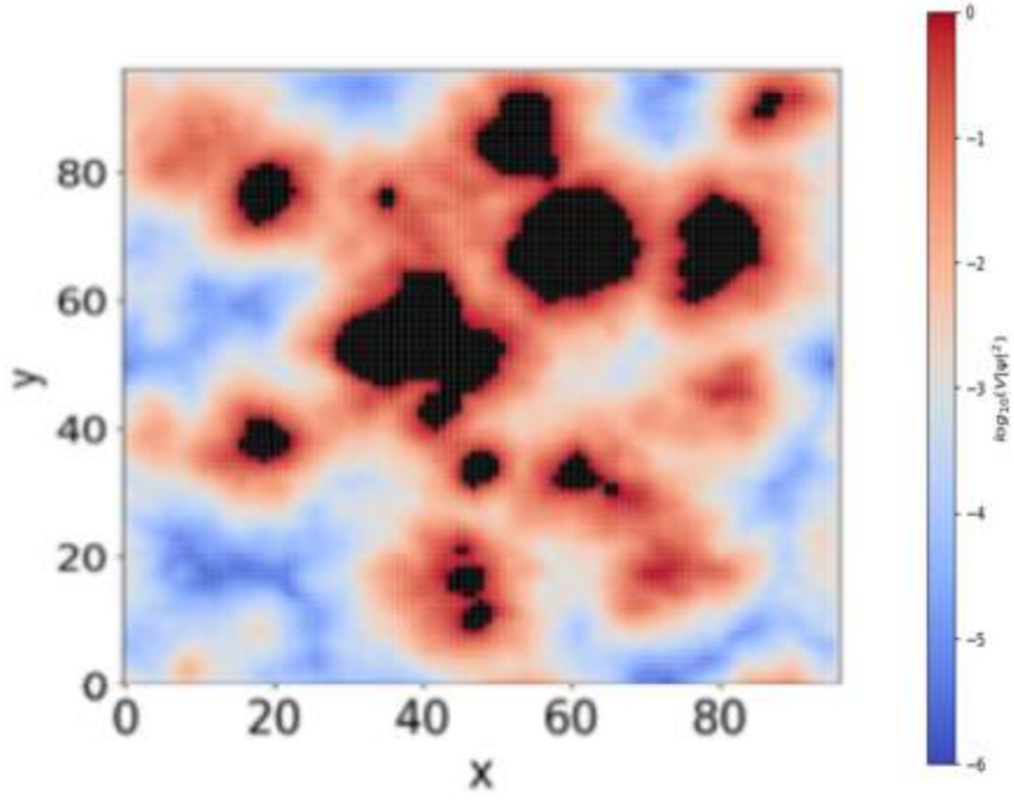

- $V(L) = (L/a)^3/(aT)$, $N_* = \sum_{x \in V} \min[V|\psi_\lambda(x)|^2, 1]$, and $\langle N_* \rangle_{L\to\infty} \propto L^{d_{\rm IR}(\lambda)}$ with T is unchanged.
- Reduce the contribution from the black region $(V\psi_\lambda^\dagger(x)\psi_\lambda(x) \geq 1)$ into 1, and add the residual contributions from the other region.
- When L becomes larger:

1. $d_{\rm IR} = 3$ if $\frac{\text{Black region}}{\text{Entire region}}$ keeps unchanged;
2. $d_{\rm IR} < 3$ if $\frac{\text{Black region}}{\text{Entire region}}$ becomes smaller.

A. Alexandru, I. Horvath, Phys. Rev.Lett. 127(2021),052303

Measure-based dimension

of the eigenvectors

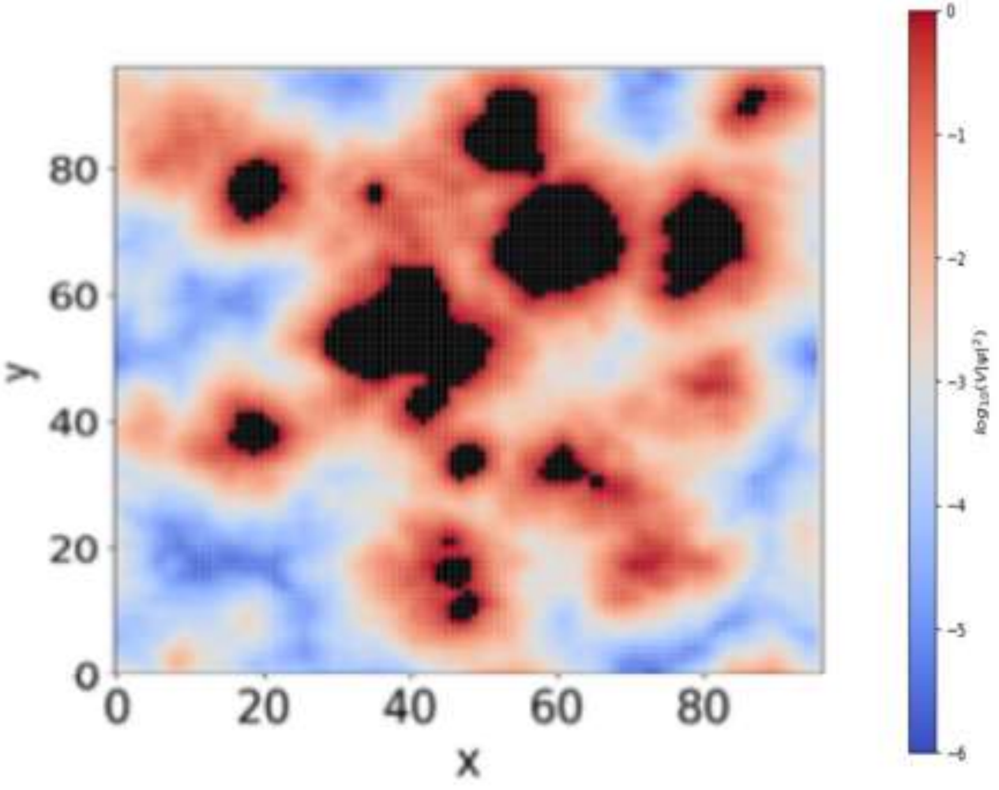

- $f_* \equiv \langle N_* \rangle / V = \sum_{x \in V} \min[\,|\psi_\lambda(x)|^2, 1/V]$
- $f_*(L)_{L\to\infty} \propto L^{d_{\rm IR}-3}$.
- When L becomes larger:

1. $d_{\rm IR} = 3$ if f_* keeps finite;
2. $d_{\rm IR} < 3$ if f_* approaches zero.

A. Alexandru, I. Horvath, Phys. Rev.Lett. 127(2021),052303

Measure-based dimension

in the 2+1 flavor case

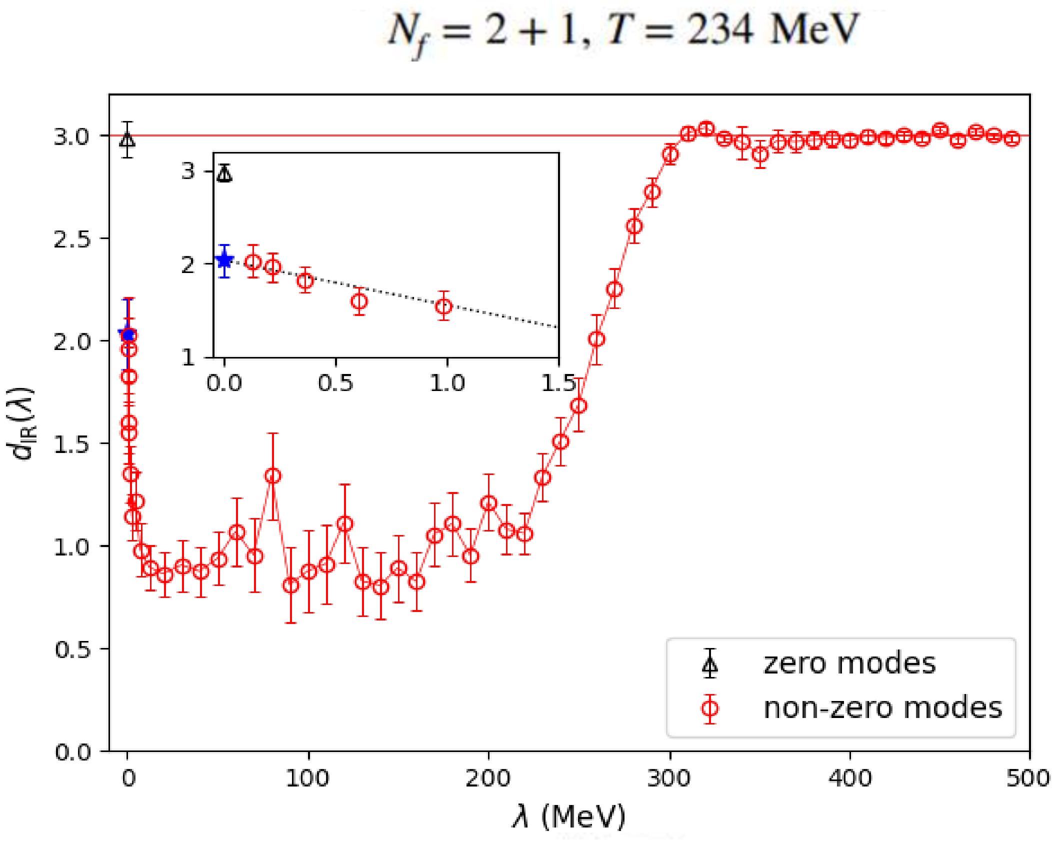

X. Meng, et.al, χQCD &CLQCD, in preparation

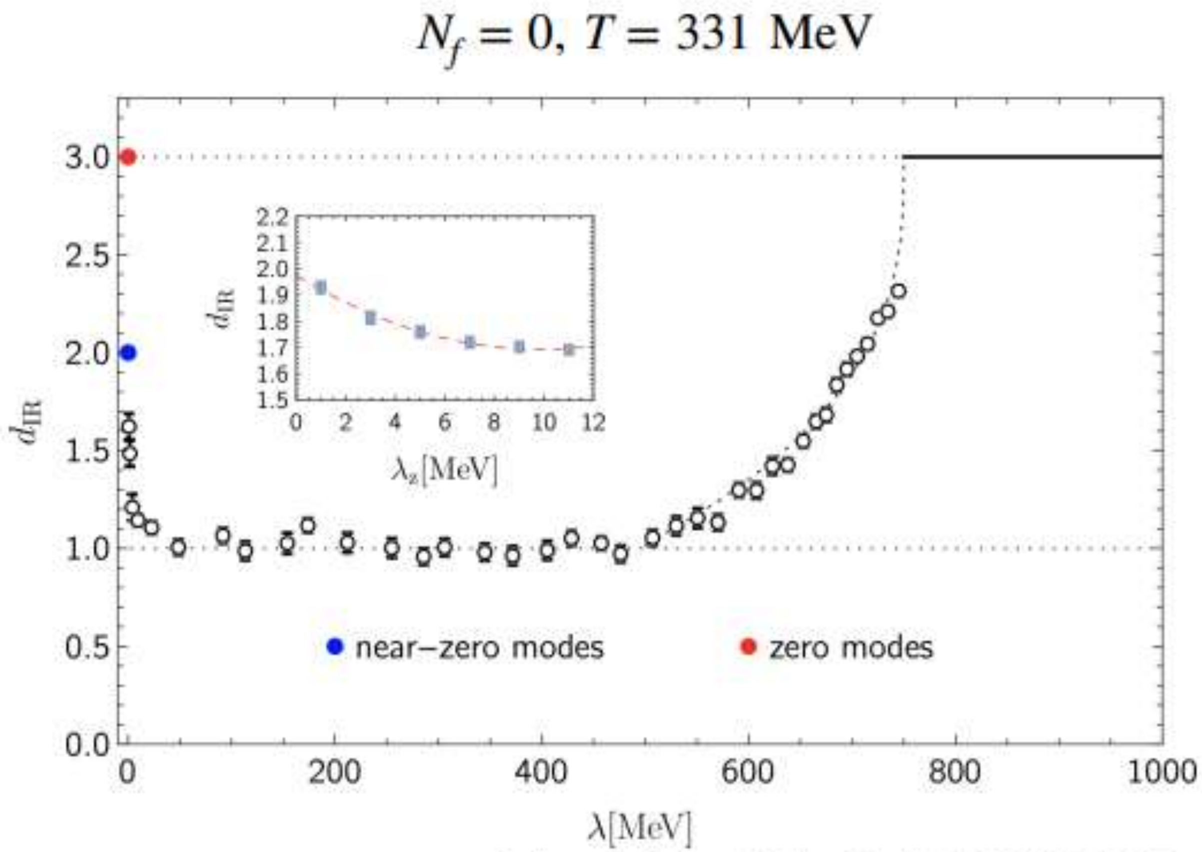

A. Alexandru, I. Horvath, Phys. Rev.Lett. 127(2021),052303

Clover ensembles

with multiple lattice spacings and pion masses

- Tadpole improved Clover fermion with stout smearing;
- Tadpole improved Symanzik gauge.
- FLAG green-star criteria can be satisfied with the present ensembles.
- Major contributors：P. Sun, L. Liu, YBY, W. Sun,…

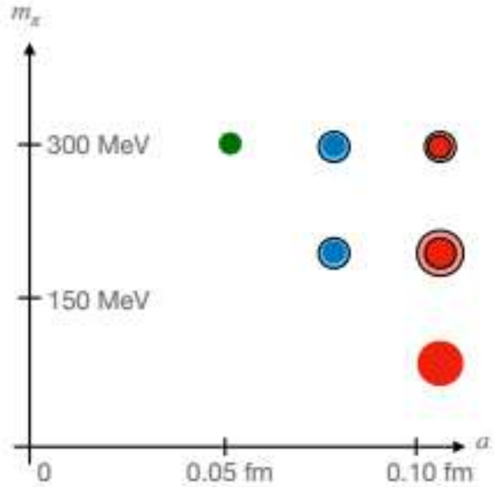

TABLE I. Lattice size $L^3 \times T$, gauge coupling $10/g^2$, bare quark masses $m^{\rm b}_{l,s,c}$, tadpole improvement factors u_0/v_0 and scale parameter w_0 of the ensembles used in this work. The bare light and starnge quark masses $m^{\rm b}_{l,s}$ with the bold font on each ensemble are the unitary quark masses, and the other values of $m^{\rm b}_{l,s,c}$ are those used for the valence quark propagators. The values $u^{\rm I}_0$ and $v^{\rm I}_0$ are the tadpole improvement factors used in the gauge and fermion actions, respectively; and u_0, v_0, w_0a are those measured from the realistic configurations generated using the Paramters here.

	C11P29Ss	C11P29S	C11P29M	C11P22M	C11P22L	C11P14L	C08P30S	C08P30M	C08P22S	C08P22M	C06P30S
$L^3 \times T$	$24^3 \times 64$	$24^3 \times 72$	$32^3 \times 64$	$32^3 \times 64$	$48^3 \times 96$	$48^3 \times 96$	$32^3 \times 96$	$48^3 \times 96$	$32^3 \times 64$	$48^3 \times 96$	$48^3 \times 144$
$10/g^2$	6.20						6.41				6.72
$m^{\rm b}_l$						**-0.2825**					
						-0.2820					
						-0.2815					
				-0.2790	**-0.2790**				**-0.2320**	**-0.2320**	
			-0.2780	-0.2780	-0.2780			-0.2307	-0.2307	-0.2307	
	-0.2770	**-0.2770**	**-0.2770**	-0.2770	-0.2770		**-0.2295**	**-0.2295**	-0.2295	-0.2295	**-0.1850**
	-0.2760	-0.2760	-0.2760				-0.2288	-0.2288			-0.1845
	-0.2750	-0.2750					-0.2275				-0.1840
$m^{\rm b}_s$	-0.2400	**-0.2400**	**-0.2400**	**-0.2400**	**-0.2400**	-0.2400	**-0.2050**	**-0.2050**	**-0.2050**	**-0.2050**	**-0.1700**
	-0.2355	-0.2355	-0.2355	-0.2355	-0.2355	-0.2355	-0.2030	-0.2030	-0.2030	-0.2030	-0.1694
	-0.2310	-0.2310	-0.2310	-0.2310	-0.2310	**-0.2310**	-0.2010	-0.2010	-0.2010	-0.2010	-0.1687
$m^{\rm b}_c$	0.4780	0.4780	0.4780	0.4780	0.4780	0.4780	0.2326	0.2326	0.2326	0.2326	0.0770
	0.4800	0.4800	0.4800	0.4800	0.4800	0.4800	0.2340	0.2340	0.2340	0.2340	0.0780
	0.4820	0.4820	0.4820	0.4820	0.4820	0.4820	0.2354	0.2354	0.2354	0.2354	0.0790
δ_τ	1.0	0.7	0.7	0.7	0.7	1.0	0.5	0.5	0.5	0.5	1.0
$n_{\rm min}$		4050	11000	4100	1000	1600	1000	2690	13500	1600	1000
$n_{\rm max}$		48000	35050	26600	5050	2200	26200	6700	36400	6060	4070
$u^{\rm I}_0$	0.855453	0.855453	0.855453	0.855520	0.855520	0.855548	0.863437	0.863473	0.863488	0.863499	0.873378
$v^{\rm I}_0$	0.951479	0.951479	0.951479	0.951545	0.951545	0.951570	0.956942	0.956984	0.957017	0.957006	0.963137
u_0		0.855440	0.855422			0.855539	0.863463				0.873373
v_0		0.951463	0.951444			0.951561	0.956971				0.963135
w_0a											

CLQCD, in preparation

Distribution

$T = 234$ MeV

at different spacial size

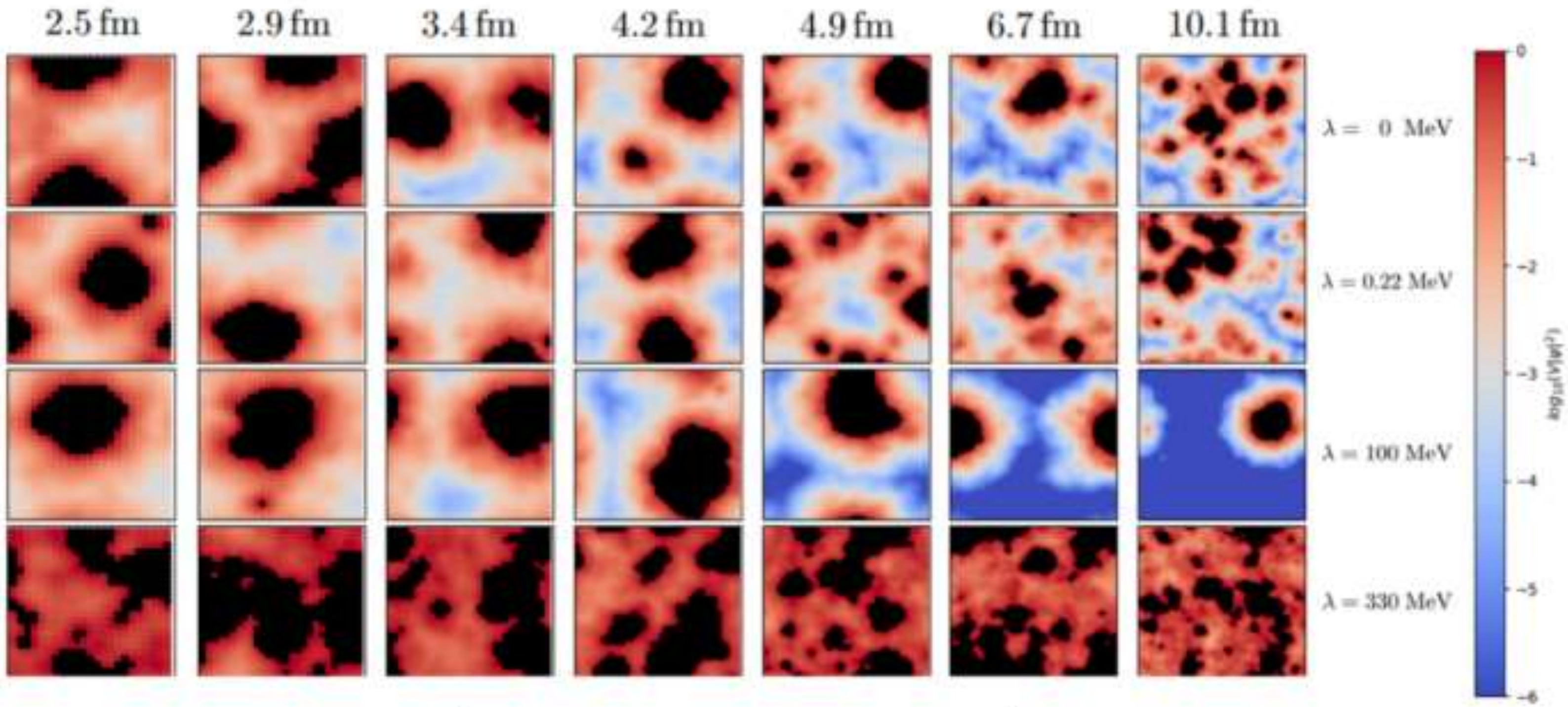

X. Meng, et.al, χQCD &CLQCD, in preparation

- Locating the position $w = w_0 \equiv \{x_0, y_0, z_0, t_0\}$ where $|\psi(\omega)|^2$ takes the maximum;
- Fix $z = z_0$ and $t = t_0$ and draw the distribution in the x-y plane.
- Black region corresponds to where $|\psi(\omega)|^2 \geq 1/V$;
- $|\psi(\omega)|^2$ is smaller when the color is colder.

Distribution

$T = 234$ MeV

at different spacial size

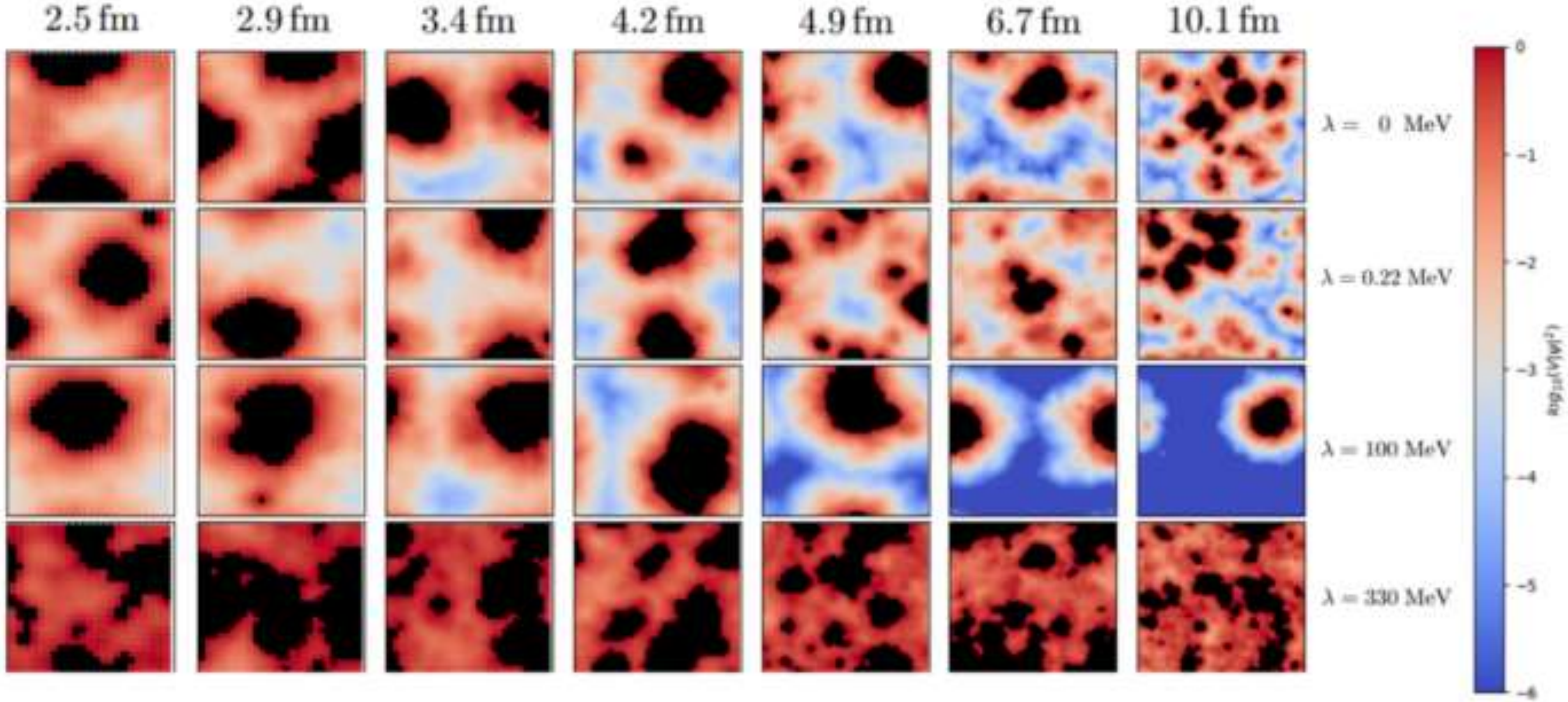

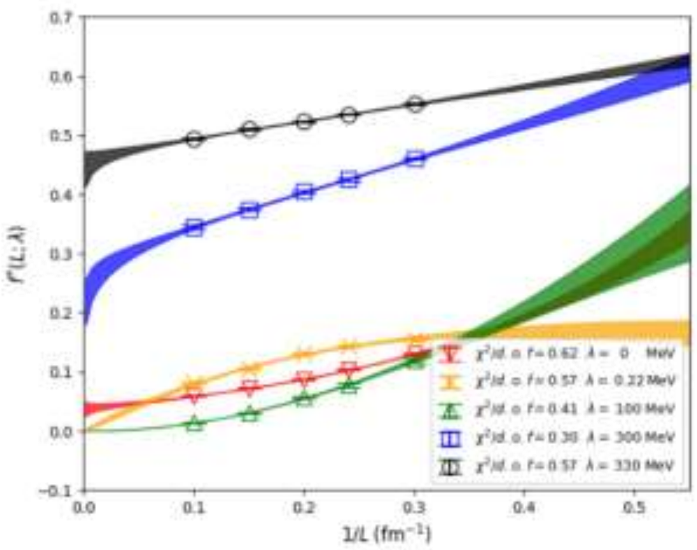

X. Meng, et.al, χQCD &CLQCD, in preparation

f_*

$T = 234$ MeV

of the eigenvectors

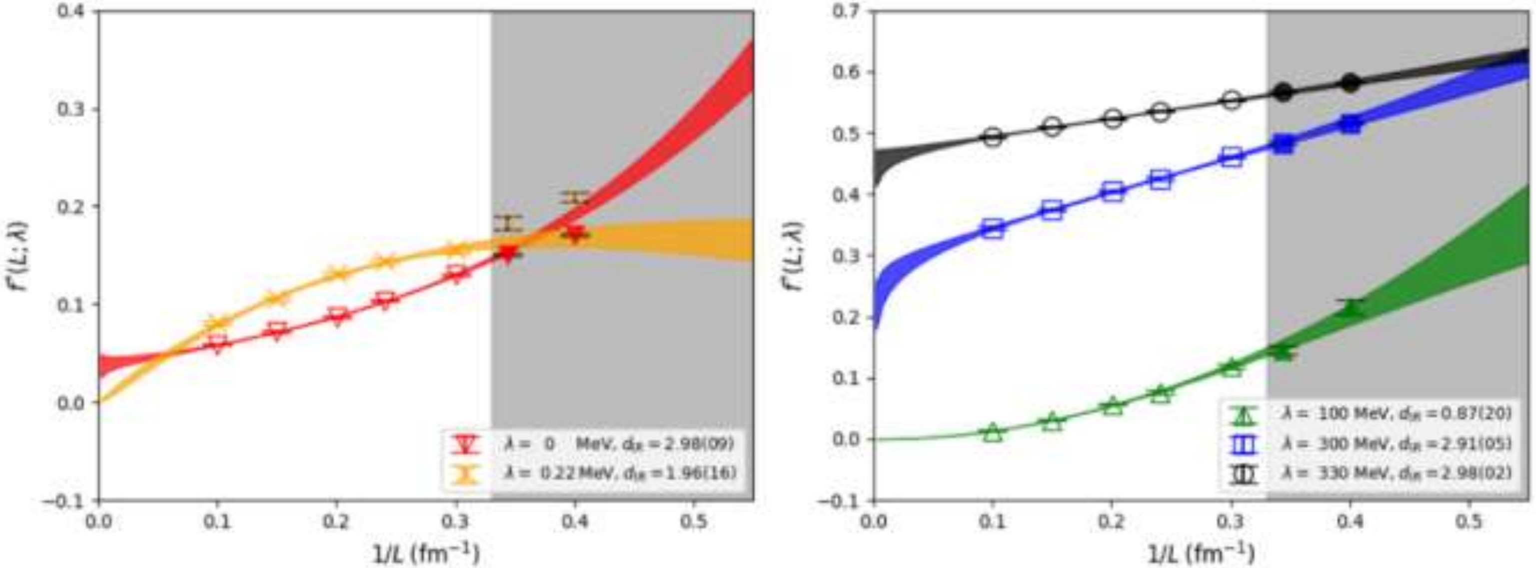

X. Meng, et.al, χQCD &CLQCD, in preparation

- we find that the following functional form $f_* = c_0(\lambda)L^{d_{\mathrm{IR}}(\lambda)-3}e^{-c_1(\lambda)/L}$ describe the data fairly well for all the λ with $L > 3.0$ fm.
- The fit is still fine when $L <$ 3.0 fm if $\lambda > 10$ MeV or so;
- But does not work for the zero modes and near-zero modes.

Measure-based dimension

$T = 234$ MeV

at different eigenvalue regions

- $f_*(\lambda)$ converges to a convex curve at $\lambda \to 0$, which is significantly different from the concave behavior of the exact zero mode with $\lambda = 0$.

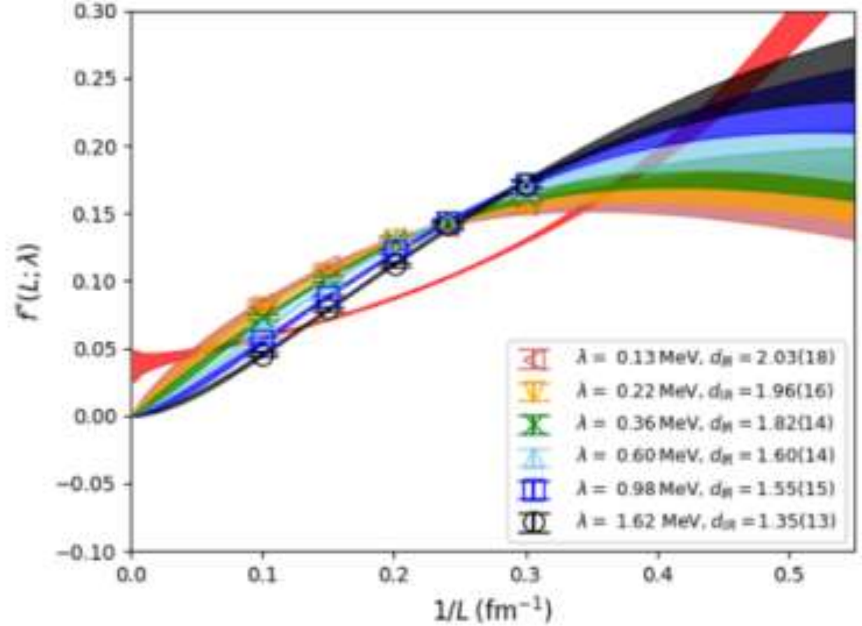

X. Meng, et.al, χQCD &CLQCD, in preparation

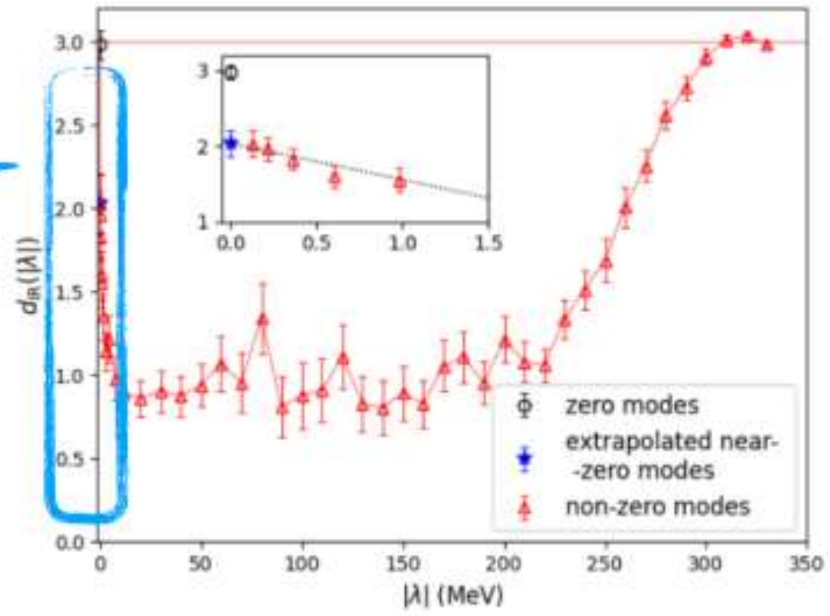

- The $f_*(\lambda \to 0)$ is larger than $f_*(\lambda = 0)$ until $L >$ 20 fm, and approaches zero when $L \to \infty$.

Measure-based dimension

$T = 234$ MeV

at different eigenvalue regions

- $f_*(\lambda)$ changes smoothly in the range of $20\ \text{MeV} \leq \lambda \leq 200\ \text{MeV}$.

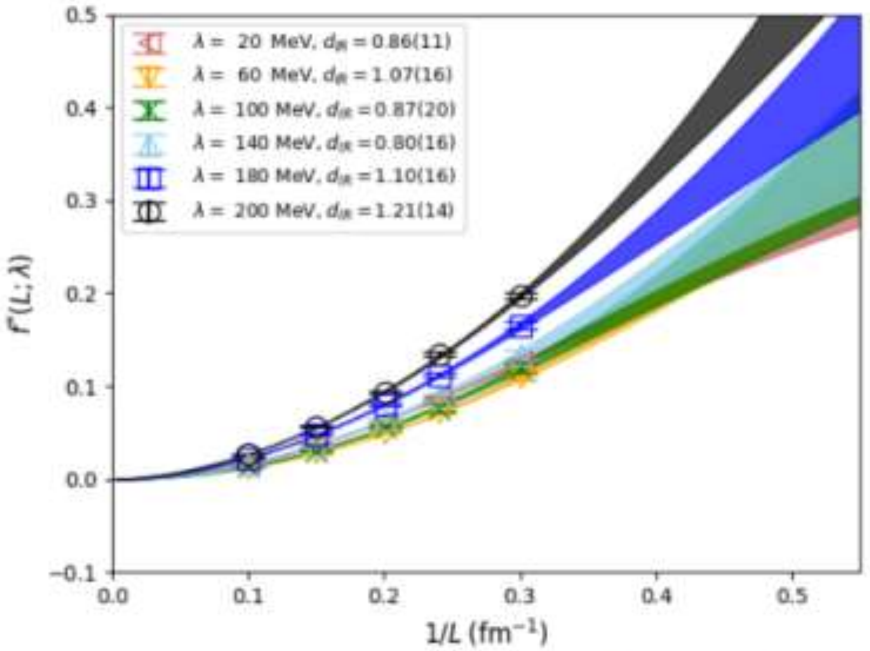

X. Meng, et.al, χQCD &CLQCD, in preparation

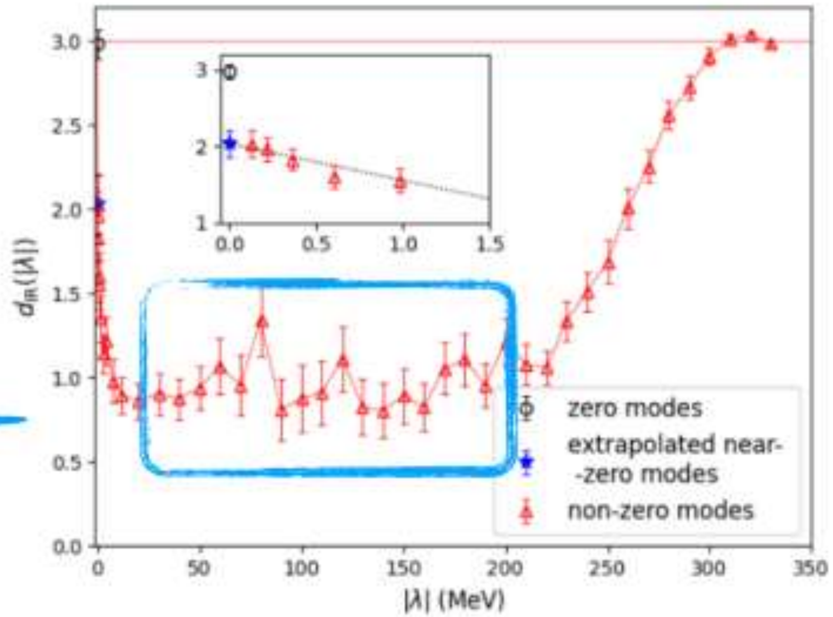

- And results in the similar effective dimension $d_{\text{IR}} = 1$.

Measure-based dimension

$T = 234$ MeV

at different eigenvalue regions

- $f_*(\lambda)$ changes also smoothly in the range of $280\ \text{MeV} \leq \lambda \leq 330\ \text{MeV}$.

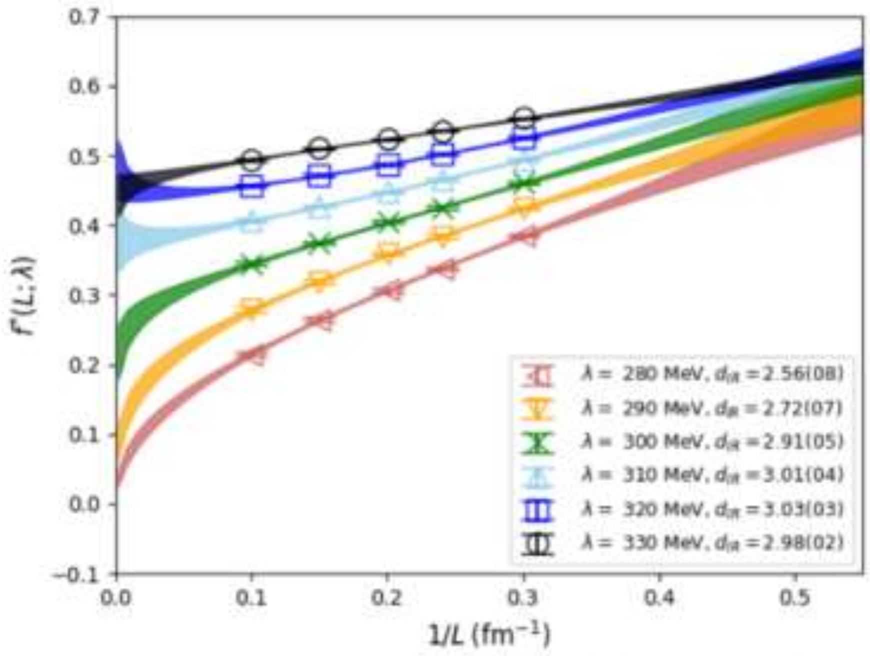

X. Meng, et.al, χQCD &CLQCD, in preparation

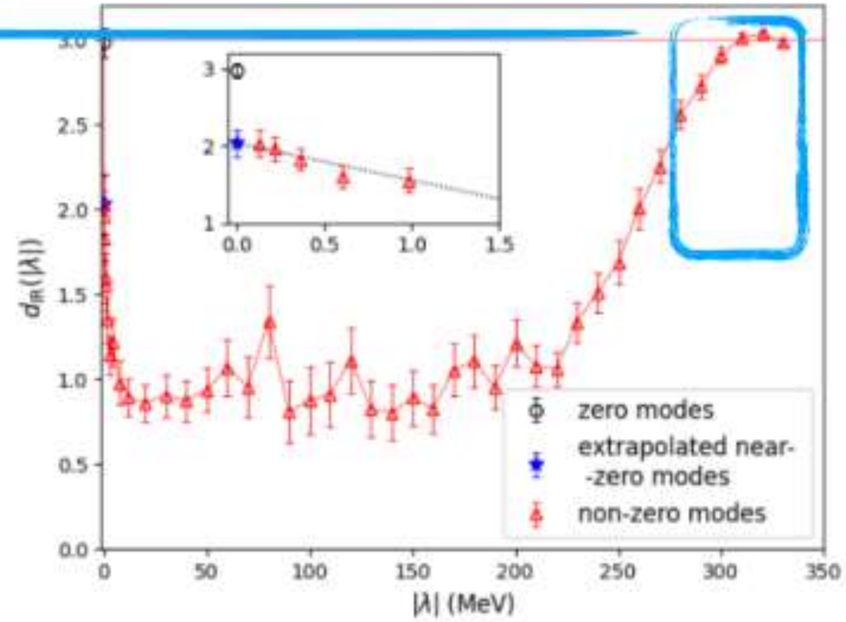

- And makes the $d_{\rm IR}$ approaches 3 without any visible discontinuity.

Distribution

at different temperatures

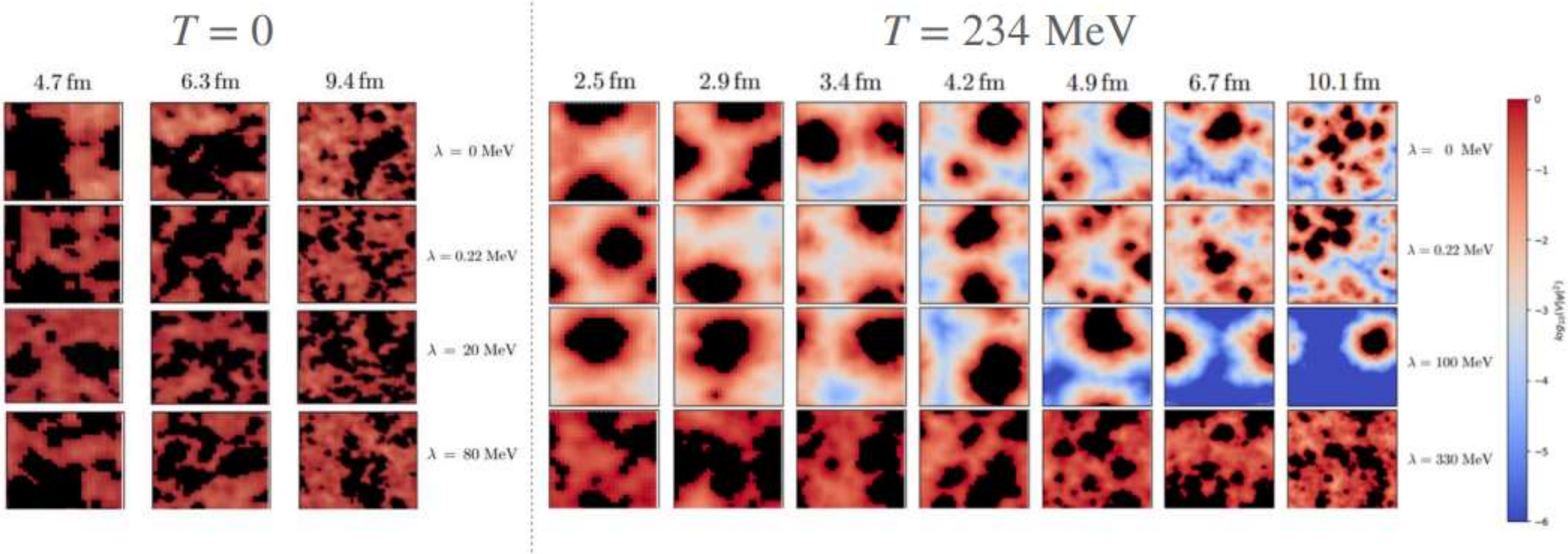

X. Meng, et.al, χQCD &CLQCD, in preparation

Summary

- We show that the important pattern of low dimensions seen in pure-glue QCD is also present in ``real-world QCD", namely in $N_f = 2+1$ ensembles with physical light and strange quark masses at a=0.105 fm:

1. $d_{\mathrm{IR}} = 3$ for the exact zero modes with $\lambda = 0$.
2. $d_{\mathrm{IR}} \to 2$ for the non-zero mode cases with $\lambda \to 0$.
3. $d_{\mathrm{IR}} = 1$ for the cases with $\lambda \in [10{,}200]$ MeV.
4. $d_{\mathrm{IR}} \to 3$ smoothly at $\lambda \sim 300$ MeV, which is lower than where $\rho(\lambda; T = 234\ \mathrm{MeV}) \sim \rho(\lambda; T = 0)$.